Phase Identification in a Series of Liquid Crystalline TPP Polyethers and Copolyethers Having Highly Ordered Mesophase Structures. 6. Structure Changes from Smectic to Columnar Phases in a Series of Copolyethers Containing Odd and Even Numbers of Methylene Units in Equal Molar Composition

Ru-Qing Zheng, Er-Qiang Chen, and Stephen Z. D. Cheng*

Maurice Morton Institute and Department of Polymer Science, The University of Akron, Akron, Ohio 44325-3909

Fengchao Xie, Donghang Yan, and Tianbai He

Polymer Physics Laboratory, Changchun Institute of Applied Chemistry, Chinese Academy of Sciences, Changchun, Jilin, 130022, P.R. China

Virgil Percec and Peihwei Chu

Department of Macromolecular Science, Case Western Reserve University, Cleveland, Ohio 44106-2699

Goran Ungar

Department of Engineering Materials, University of Sheffield, Sheffield S1 3JD, UK

Received December 3, 1998; Revised Manuscript Received March 28, 1999

ABSTRACT: A series of liquid crystalline copolyethers has been synthesized from 1-(4-hydroxy-4′-biphenyl)-2-(4-hydroxyphenyl)propane and different α,ω-dibromoalkanes [coTPP(*n*/*m*)]. In this report, coTPPs having $n = 5, 7, 9, 11$ and $m = 12$ are studied, which represent copolyethers having both varying odd number and a fixed even number of methylene units. The compositions were fixed at an equal molar ratio (50/50). These coTPPs(*n*/*m*) show multiple phase transitions during cooling and heating in differential scanning calorimetry experiments. The undercooling dependence of these transitions is found to be small, indicating that these transitions are close to equilibrium. Although the coTPPs possess a high-temperature nematic (N) phase, the periodicity order along the chain direction is increasingly disturbed when the length of the odd-numbered methylene units decreases from $n = 11$ to 5. In the coTPPs(5/12, 7/12, and 9/12), wide-angle X-ray diffraction experiments at different temperatures show that, shortly after the N phase formation during cooling, the lateral molecular packing improves toward a hexagonal lattice, as evidenced by a gradual narrowing of the scattering halo. This process represents the possible existence of an exotic N phase, which serves as a precursor to the columnar (Φ_H) phase. A further decrease in temperature leads to a Φ_H phase having a long-range ordered, two-dimensional hexagonal lattice. In coTPP(11/12), the phase structures are categorized as highly ordered and tilted, smectic and smectic crystal phases, similar to homoTPPs, such as the smectic F (S_F) and smectic crystal G (SC_G) phases. An interesting observation is found for coTPP(9/12), wherein a structural change from the high-temperature Φ_H phase to the low-temperature S_F phase occurs. It can be proven that, upon heating, the well-defined layer structure disappears and the lateral packing remains hexagonal. The overall structural differences in this series of coTPPs between those of the columnar and highly ordered smectic phases are related to the disorders introduced into the layer structure by the dissimilarity of the methylene unit lengths in the comonomers.

Introduction

In our previous reports on the phase identification in a series of main-chain liquid crystalline (LC) polyethers synthesized from 1-(4-hydroxy-4′-biphenyl)-2-(4-hydroxyphenyl)propane and α,ω-dibromoalkanes [TPP(*n*)], the following phases were found: highly ordered smectic F (S_F), smectic crystal G (SC_G), and H (SC_H) phases.[1−3] The identification has been confirmed via molecular motion studies of each of these phases using solid-state carbon-13 nuclear magnetic resonance (NMR).[4] It has also been found that several new phases in some of these TPPs can be surface induced and stabilized, which are originally metastable in the bulk samples.[5,6] The phase structures and transition behaviors of TPPs with odd- and even-numbered methylene units are different. For example, TPPs($n = 5$, 7, and 9) exhibit the following phase behavior:[1,2]

$$\text{glassy state} \leftrightarrow SC_G \leftrightarrow S_F \leftrightarrow N \leftrightarrow I$$

whereas for TPP($n = 11$), the phase transition sequence is as follows:[2]

$$\text{glassy state} \leftrightarrow SC_H \leftrightarrow SC_G \leftrightarrow S_F \leftrightarrow N \leftrightarrow I$$

and the phase behavior of TPP($n = 12$) is[3]

$$\text{glassy state} \leftrightarrow K_2 \leftrightarrow K_1 \leftrightarrow SC_H \leftrightarrow SC_G \leftrightarrow S_F \leftrightarrow I$$

These transitions are all at thermodynamic equilibrium. It is important to note that even though S_F, SC_G,

* To whom the correspondence should be addressed.

10.1021/ma9818782 CCC: $18.00
Published on Web 05/13/1999

and SC_H phases are found in both odd- and even-numbered TPPs, TPPs($n = 5$, 7, 9, and 11) exhibit a N phase whereas TPP($n = 12$) does not. Moreover, the S_F and SC_G phases in TPPs($n = 5$, 7, 9, and 11) possess molecular axes that are tilted with respect to the fiber direction as observed via wide-angle X-ray diffraction (WAXD) fiber patterns.[1,2] For example, in the S_F phase, the tilt angle is between 14° for TPP($n = 7$) and 7° for TPP($n = 11$), whereas the SC_G phase ranges from 16° for TPP($n = 7$) to 5° for TPP($n = 11$).[1,2] No tilt angle is found in the SC_H phase of TPP($n = 11$).[2] On the other hand, TPP($n = 12$) exhibits phases containing molecular axes parallel to the fiber direction.[3] Finally, TPP($n = 12$) possesses two crystalline phases, K_1 and K_2 at low temperatures, which do not exist in TPPs($n =$ odd).[3] The thermodynamic transition properties (transition temperatures and enthalpies) are also different in these TPPs.[1−3]

Columnar (Φ) phases were first studied in low molecular mass discotic molecules, where the molecular geometry usually requires not only a disklike core but also flexible tails connected to the core (typically, at least six methylene units are required) for the existence of a Φ phase.[7,8] The discotic molecules may possess either an ordered (Φ_O) or a disordered (Φ_D) structure along the disk-stacking direction, although even the Φ_O phase has no long-range order along this direction.[9] The lateral packing, on the other hand, involves three major types of two-dimensional lattice arrays: hexagonal (Φ_H), rectangular (Φ_R), and oblique (Φ_{OB}). These packings can be well defined by two-dimensional symmetries on the basis of crystallographic analyses. Several nondiscotic liquid crystal molecules have also later been reported demonstrating Φ phases.[10−12]

Introducing the Φ phase concept to describe phase behaviors in thermotropic linear flexible or semiflexible polymers requires further discussion. Specifically, incorporating comonomers with different methylene unit lengths into a main-chain LC polymer containing mesogenic groups, such as TPPs, may lead to an aperiodicity along the molecular backbone. This chemical dissimilarity may result in a two-dimensional hexagonal ordered structure (Φ_H).[13] We have therfore intentionally designed copolymers that generate phase transitions involving less ordered structures. A series of coTPPs were prepared with the following chemical structures:

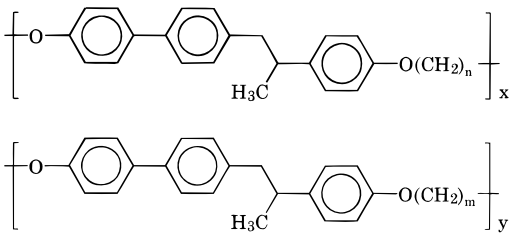

The coTPPs studied have a fixed even number ($m = 12$) and varying odd numbers ($n = 5$, 7, 9, and 11) of methylene units. The compositions (x/y) were fixed at an equal molar ratio (50/50). The effect of the comonomer length on the phase structure and transition behavior is investigated and reported in this publication.

Experimental Section

Materials. A series of coTPPs($n/m = 5/12$, 7/12, 9/12, and 11/12) were synthesized by random copolymerization of 1-(4-hydroxy-4′-biphenyl)-2-(4-hydroxyphenyl)propane with 1,5-dibromopentane, 1,7-dibromoheptane, 1,9-dibromononane, 1,-11-dibromoundecane, and 1,12-dibromododecene. The detailed synthetic procedure of homoTPPs has been reported in an earlier publication.[14] The number-average molecular weight (M_n) was determined via gel permeation chromatography (GPC) based on polystyrene standards and ranged from 20 000 to 30 000 g/mol.

Instruments and Experiments. DSC experiments were carried out in a Perkin-Elmer DSC-7. The temperature and heat flow scales at different cooling and heating rates (2.5−40 °C/min) were calibrated using standard materials. A typical DSC sample size ranged from 1.0 to 3.0 mg. The samples were heated above their melting temperatures for 2 min and then cooled at different rates. Subsequent heating was performed at a rate faster than or equal to the prior cooling. The cooling and heating scans were used to determine the transition temperatures by measuring the onset temperatures on the high- and low-temperature sides of the transition peaks, respectively.

WAXD reflection experiments were conducted with a Rigaku 12 kW rotating-anode generator (Cu Kα) coupled with a Geigerflex D/max-RB diffractometer (with radius of 185 mm). The X-ray beam was line focused and monochromatized using a graphite crystal. The beam size was controlled by the slit system (a divergence slit of 0.5°, a receiving slit of 0.15 mm, and a scattering slit of 0.5°). The reflection peak positions and widths were calibrated with silicon crystals of known crystal size in a high angle region ($2\theta > 15°$) and silver behenate in a low angle region ($2\theta < 15°$). The angular deviation measured in WAXD was ±0.05° with an instrumentation function of 0.03°. A hot stage in conjunction with the diffractometer was used to study the structural changes during phase transitions. The temperature was controlled to better than ±1 °C. Film samples with a thickness of approximately 0.1 mm were prepared for the WAXD powder experiments and were scanned in a 2θ region between 2° and 30°. Background scattering was recorded and subtracted from the WAXD patterns.

Fibers were spun from the N phase in order to identify the phase structures. The fibers were quenched to room temperature after spinning; the typical fiber diameter was 30 μm. The as-spun fibers were used to carry out heating experiments on an imaging plate (Rigaku automated X-ray imaging system with 3000 × 3000 pixel resolution) with a built-in hot stage. A 30 min exposure was required to obtain a high-quality WAXD fiber pattern. The same calibration procedure described previously was followed. The unit cell determination procedure was based on the reciprocal lattice approach. Computer refinement was performd to achieve the fit with the least error between experimental and calculated data based on a continuous refinement program established in our laboratory. Correlation lengths can be estimated by using the Scherrer equation, wherein the peak width at half-height of each reflection is reciprocally proportional to the correlation length perpendicular to the reflection planes.

Phase morphology was examined via polarized light microscopy (PLM) (Olympus BH-2) coupled with a Mettler hot stage (FP-90). Both isothermal and nonisothermal experiments were performed. The films were obtained using small amounts of coTPPs which were melt-pressed between two glass slides in order to study the LC morphological changes at different temperatures.

LC morphologies were also studied using a JEOL, JEM-120 transmission electronic microscope (TEM) with an accelerating voltage of 120 kV. CoTPP thin films were solution cast on amorphous carbon-coated surfaces at a concentration of 0.1% (w/w) in tetrahydrofuran (THF). Following the solvent evaporation, the films were heated and held in the N phase for 15 h followed by slow cooling. Several samples were mechanically sheared and quenched. The films were then coated with platinum and carbon. To determine the lateral packing structure and chain molecular direction, the unsheared and sheared samples were examined by electron diffraction (ED) experiments using TEM.

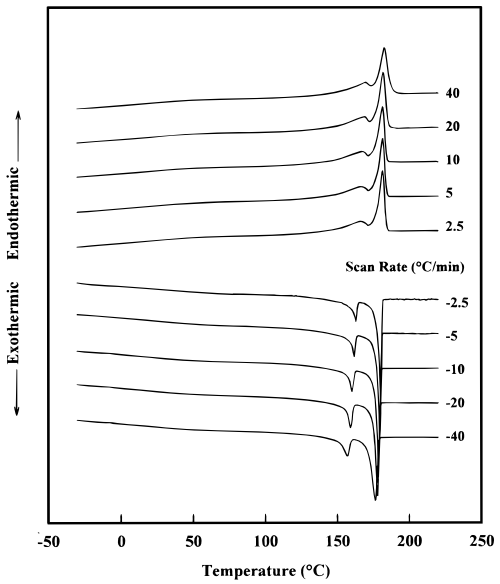

Figure 1. Set of DSC curves of coTPP(7/12) for different cooling and subsequent heating rates.

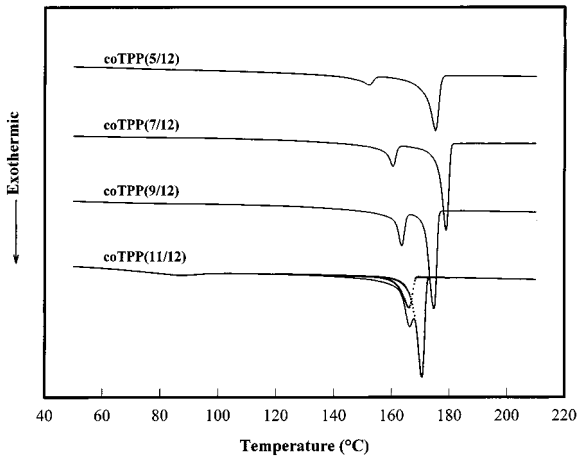

Figure 2. Set of DSC cooling curves for four coTPPs at 10 °C/min with a peak separation for coTPP(11/12).

Results and Discussion

Thermal Transitions in coTPPs. Figure 1 contains both sets of heating and cooling DSC curves of coTPP-(7/12) as an example; multiple exothermic and endothermic peaks were observed. Similar to homoTPPs,[1−3] the transition enthalpies exhibit almost no heating and cooling rate dependence, implying that the transitions are near thermodynamic equilibrium. The undercooling of the onset transition temperatures is only a few degrees, as observed for the scans ranging from 2.5 to 40 °C/min. Similar observations have been found in other coTPPs. The equilibrium transition temperatures were obtained by extrapolating the heating and cooling rates to 0 °C/min. (The extrapolated transition temperature is typically 1−2 °C higher than that at 2.5 °C/min during cooling.)

Figure 2 describes the cooling behavior of these four samples scanned at 10 °C/min. Two major exothermic peaks were found, which get closer to each other as the odd number of methylene units increases. The high-temperature transition peaks for coTPPs(5/12, 7/12, and 9/12) are relatively broad compared to that of coTPP-(11/12). Two phase transitions are observed for coTPPs-(5/12 and 7/12) and three for coTPP(9/12), one of which includes a very broad transition below 100 °C. Three transition processes are also observed in coTPP(11/12), with the onset low-temperature transition at approximately 100 °C. Detailed thermodynamic properties will be discussed following the identification of the phase structures.

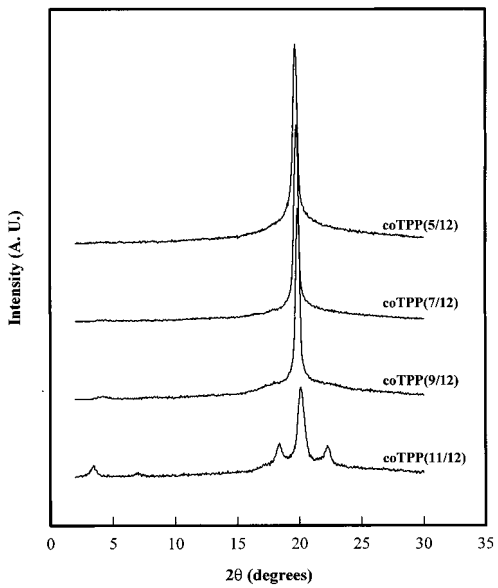

Figure 3. WAXD powder patterns of four coTPPs at 40 °C after the samples were cooled from the isotropic melt at 2.5 °C /min.

Phase Structure Identification at Room Temperature. Figure 3 describes the WAXD powder patterns for the four copolyethers at room temperature. CoTPP(11/12) results in a WAXD powder pattern completely different from the others, showing three reflections at 2θ of 18.3°, 20.2°, and 22.3° (d spacings of 0.48, 0.44, and 0.40 nm), respectively. At the low angle region, the first- and second-order reflections with 2θ values of 3.5° and 7.0° (d spacings of 2.50 and 1.25 nm) are also evident, which may represent the layer ordering. However, the low angle reflections become less intense when the dissimilarity between the methylene unit lengths increases. In the WAXD pattern of coTPP(9/12), only a weak low angle reflection at a 2θ of 4.1° (d spacing of 2.16 nm) is found. The WAXD pattern of coTPP(9/12) in the wide angle region shows a sharp reflection at a 2θ of 19.9° (d spacing of 0.45 nm) and two very weak reflections similar to those of coTPP(11/12) on both sides of the major reflection. CoTPPs(5/12 and 7/12) exhibit quite different WAXD powder patterns from their corresponding homoTPPs.[2,3] In the wide angle region of coTPP(7/12), one sharp and intense reflection at a 2θ of 19.8° (d spacing of 0.45 nm) can be seen. The two very weak reflections only show residual traces and cannot be clearly identified. In coTPP(5/12), only one sharp and intense reflection at 2θ of 19.8° (d spacing of 0.45 nm) can be observed, indicating a possible hexagonal lateral chain-packing scheme in a two-dimensional array. The low angle reflection seen in coTPPs(9/12 and 11/12) is almost unobservable in coTPP(7/12) and is completely absent in coTPP(5/12).

Figure 4a−d illustrates the WAXD fiber patterns for these coTPPs at room temperature. The fiber pattern of coTPP(11/12) demonstrates three lateral reflections at 2θ of 18.3°, 20.2°, and 22.3° on the equator and in quadrant, corresponding to the ($\bar{2}$01), (110), and (201) reflections which are similar to those of the homoTPPs

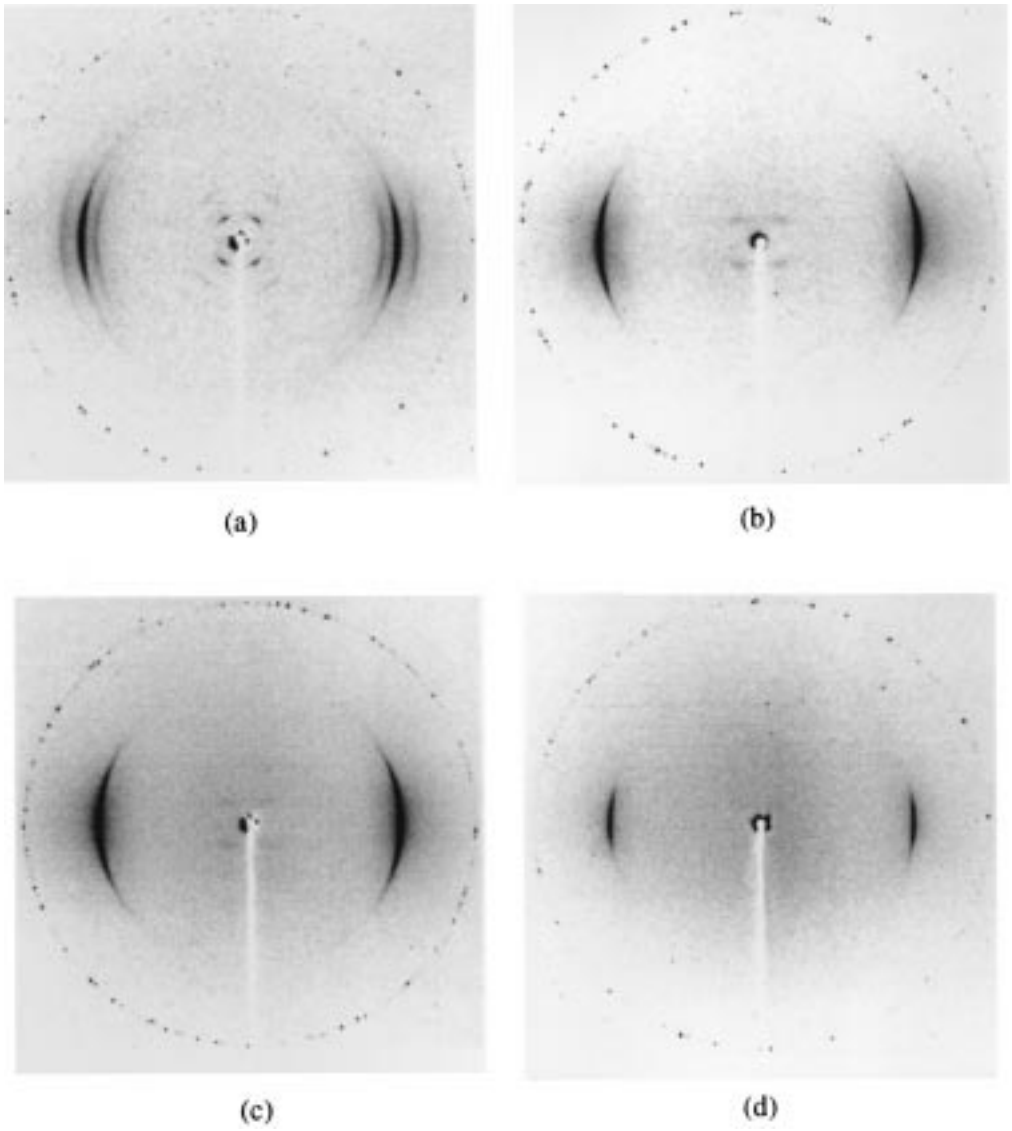

Figure 4. WAXD fiber patterns of four coTPPs at room temperature: (a) coTPP(11/12), (b) coTPP(9/12), (c) coTPP(7/12), and (d) coTPP(5/12).

(monoclinic lattices).[1−3] The first- and second-order reflections in the low angle region are sharp, and the layer structures are thus well defined. They are located in the quadrant at an angle of 37° from the fiber direction and are assigned as the (001) and (002) reflections. The structure analyses show that this copolyether possesses a monoclinic unit cell of $a = 1.12$ nm, $b = 0.52$ nm, $c = 3.10$ nm, and $\beta = 127°$. Note that the tilting of the unit cell is toward one side, which may lead to the split of the (110) and (200) reflections and a substantial broadening of the peak at a 2θ of 20.2°. Similar observations have been reported in the homoTPPs.[1−3] Therefore, a hexagonal packing can be identified perpendicular to the molecular axis, and coTPP(11/12) can be assigned as a SC_G phase. The layer spacings, c, for the homoTPPs($n = 11$ and 12) in the low-temperature phases are 2.81 and 3.22 nm, respectively, indicating that coTPP(11/12) is intermediate of these two homopolymers, with a layer spacing of 3.10 nm. The β value of 127° of coTPP(11/12) is also intermediate between 130° for TPP($n = 11$) and 121° for TPP($n = 12$). However, both homoTPPs possess the SC_H phase with a rectangular lateral packing, whereas coTPP(11/12) exhibits a hexagonal one. This may reveal that the copolymerization and the difference in methylene unit lengths disturb the lateral packing by decreasing the order from the rectangular to hexagonal two-dimensional arrays (i.e., increasing the symmetry).

The fiber pattern of coTPP(9/12) shows a sharp reflection on the equator at a 2θ of 19.9° (Figure 4b). This reflection is attributed to a hexagonal lattice in a two-dimensional array perpendicular to the molecular axis; therefore, the (110) plane can be indexed on the basis of a rectangular lattice. The layer reflection for coTPP(9/12) is still spotlike but is lower in intensity and more diffuse than that of coTPP(11/12). This layer reflection is tilted 43° with respect to the fiber direction. The other high-angle reflections such as the ($\bar{2}$01) and (201) planes are weak, which may be associated with the weak (00l) layer reflection. However, the (110) reflection, which is unrelated to the layer spacing, is still sharp. Therefore, this structure fits the classical definition of an S_F phase.[9,15] A monoclinic unit cell can be deduced with $a = 1.22$ nm, $b = 0.52$ nm, $c = 2.95$ nm, and $\beta = 133°$. Compared to the unit cell dimensions of coTPP(11/12), the lateral dimensions have increased, indicating a gradual loosening of the lateral packing in coTPP(9/12).

In the coTPP(7/12) fiber pattern (Figure 4c), the sharp equatorial reflection appears at a 2θ of 19.9° (d spacing

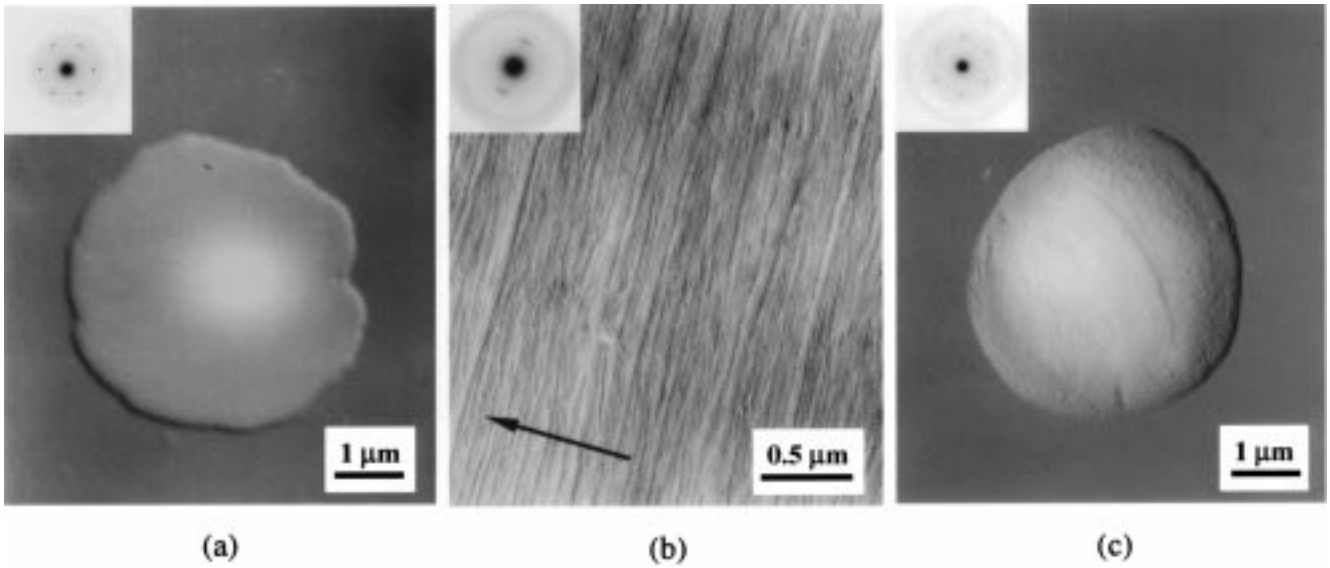

Figure 5. TEM observations: (a) unsheared coTPP(7/12), (b) mechanically sheared coTPP(7/12), and (c) unsheared coTPP(11/12). The arrow represents a shear direction.

of 0.45 nm). Another weak but sharp equatorial reflection is found outside the silicon ring at a 2θ of approximatly 35°, corresponding to a d spacing of 0.26 nm (not shown in Figure 4c). The ratio of these two d spacings yields a value of $\sqrt{3}$, which is characteristic of a hexagonal lateral packing. On the other hand, only weak and diffuse streaks in the quadrant are observed in the low angle region, and it follows that the defects existing in the layer structure are mainly due to the mismatch of the mesogenic groups along the layer normal and/or fiber direction. In this case, any (hkl, $l \neq 0$) reflection that is associated with the layer structure is difficult to observe. This leads to the reflection of the (110) planes on the equator. On the basis of the fact that only a two-dimensional array exists in this copolymer, the classical definition of the highly ordered smectic phases does not hold for the phase structure of coTPP-(7/12). A Φ_H phase may be assigned, where the molecular chain orientation is parallel to the fiber direction. However, the weak and diffuse streaks remain, suggesting that the residual layer structure still exists in this copolymer.

The fiber pattern of coTPP(5/12) (Figure 4d) represents a single, sharp lateral reflection on the equator. No layer reflections can be experimentally observed, indicating that the ordered layer structure is almost destroyed, leading to a disappearance of the (hkl, $l \neq 0$) reflections in the fiber pattern. Again, this phase can be assigned as a Φ_H phase.

Figure 5a shows a TEM lamellar domain morphology obtained from a thin film of coTPP(7/12). The ED pattern attached to this figure shows a hexagonal lattice with a d spacing of 0.45 nm, which is perpendicular to the chain direction. The morphology and ED pattern of a mechanically sheared coTPP(7/12) are shown in Figure 5b, which is similar to the WAXD fiber pattern (Figure 4c). From ED pattern of coTPP(11/12) (Figure 5c), the hexagonal lattice is again evident with the [001] zone, and this agrees with the SC_G phase assignment as determined by WAXD experiments. For these four coTPPs, the calculated lattice dimensions based on ED patterns are consistent with the WAXD results.

On the basis of these experimental observations, one may find a smectic crystal phase with a three-dimensionally ordered SC_G structure in coTPP(11/12), a highly ordered smectic S_F phase in coTPP(9/12), but a columnar phase with a two-dimensionally, lateral ordered structure in coTPPs(5/12 and 7/12), due solely to the increase of mismatch of the spacer lengths in the two comonomers.

Phase Transformation Sequences. In addition to the phase structure determinations at room temperature, it is important to recognize the phase transition sequences and their structural evolution as a function of temperature. Figure 6a shows the WAXD powder patterns for coTPP(7/12) at different temperatures during cooling. The heating WAXD experiments exhibit almost identical reflection patterns, and therefore, only the cooling results are discussed. At the highest transition temperature of approximately 180 °C, there is a slight but sudden shift of the scattering halo toward a higher 2θ value. The halo maximum has a 2θ of approximately 18°, with a corresponding d spacing of approximately 0.5 nm attributed to the average distance between chain molecules in the lateral packing. No sharp Bragg reflection was observed during this transition. The sudden shift of the scattering halo represents a N−LC transition from the isotropic melt, which is the case in many main-chain LC polymers,[12,16−18] including the series of homoTPPs.[1−3] The scattering halo narrows with a further decrease in temperature. Upon reaching approximately 160 °C, a sharp Bragg reflection appears at a 2θ of 19.0°, corresponding to the formation of a new phase (Φ_H). Also, upon cooling, the peak intensity gradually increases, but once 70 °C is reached, the intensity remains constant; the halo d spacing continuously decreases due to the thermal contraction. The existence of long-range order in the two-dimensional lateral packing of this phase can be clearly identified.

The WAXD powder patterns of coTPP(7/12) (Figure 6b) recorded during cooling at 5 °C intervals show a temperature region possessing a narrowing process of the halo from 180 to 165 °C. Note that this temperature region corresponds to the broadening shoulder of the high-temperature transition peak observed in the DSC experiments (Figures 1 and 2). Similar narrowing behavior was found in coTPP(5/12) from 175 to 155 °C and in coTPP(9/12) from 175 to 165 °C. Parts a and b of Figure 7 describe the temperature dependence of the d

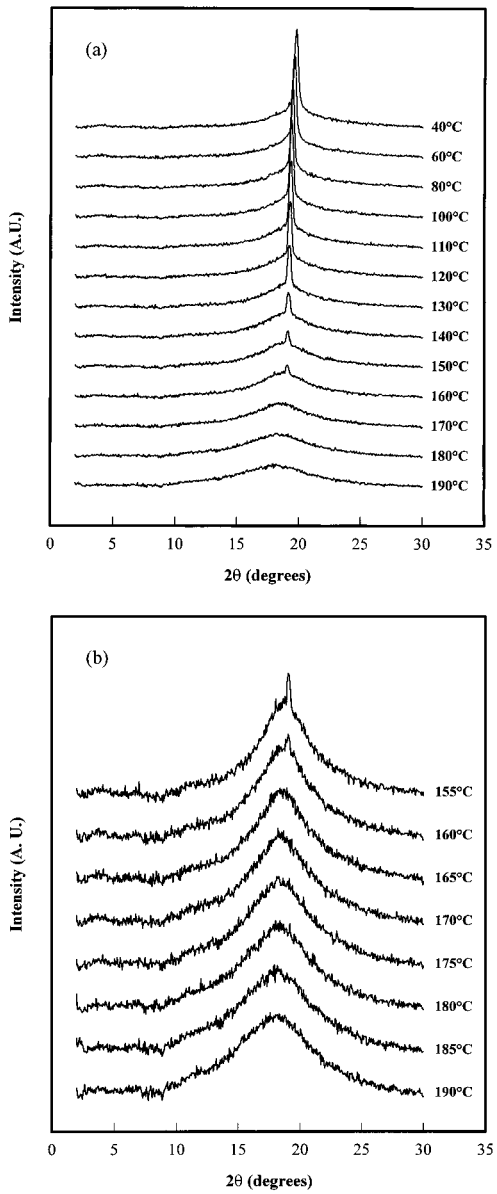

Figure 6. Two sets of WAXD powder patterns for coTPP(7/12): (a) at different temperatures during cooling at 2.5 °C/min and (b) between 190 and 150 °C at 5 °C intervals.

spacing and the correlation length of the scattering halo calculated from the WAXD patterns, respectively. It is evident that the I → N transition is accompanied by a shift of the halo *d* spacing. Once the N phase has formed, the scattering halo continues to narrow as illustrated by an increase in the correlation length. This implies that in this temperature region the lateral packing of the copolymer chains gradually improves toward a hexagonal array during cooling. Some examples of low molecular weight LC molecules have shown to possess higher order in N phases, such as hexagonal and icosahedral symmetries, and are named exotic N phases.[9] Moreover, no low angle Bragg reflection is observed in Figure 6b, differing from the homopolymers.[1−3] We speculate that this indicates the presence of a precursor to the Φ_H phase formation.

Further decrease in temperature brings about the sharp Bragg reflection at a 2θ of 19.0°, indicating that a long-range order lateral packing develops and is retained as a two-dimensional hexagonal array. This process is associated with the second DSC exothermic

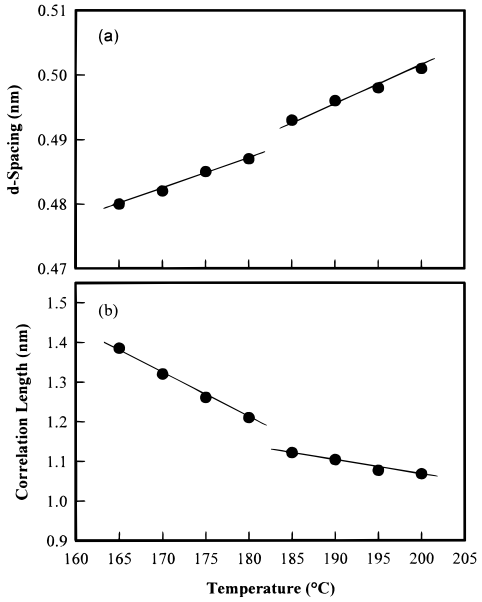

Figure 7. Relationship of (a) the *d* spacing of the scattering halo and (b) the correlation length of coTPP(7/12) with respect to temperature.

peak found on cooling, as in Figures 1 and 2. One expects the coTPP(5/12) to be an even better representative of the Φ_H phase, since it is the most dissimilar with respect to the methylene unit lengths.

The PLM observations also support the phase assignment. Figure 8 presents the morphologies of coTPP(7/12) at different temperatures. The N phase appears at 180 °C as observed by the two and four brushes, as shown in Figure 8a, revealing the LC defects of $S = \pm^1/_2$ and ± 1. With decreasing temperature, the change in LC texture is still visible (Figure 8b), which implies that the exotic N phase also affects the LC morphology. Figure 8c describes the morphology of a Φ_H phase. It seems that some chains are oriented parallel to the light beam and generate the extinction area; others exhibit banded textures that are "fingerprints" of the Φ_H phase with a column direction more or less parallel to the substrate surface. Therefore, the phase transformation sequence of coTPP(7/12) (and also for 5/12) is

$$\text{glassy state} \leftrightarrow \Phi_H \leftrightarrow \text{N} \leftrightarrow \text{I}$$

CoTPP(11/12) exhibits a completely different phase transition behavior, which is similar to that of homopolymers.[1−3] Figure 9 shows a set of WAXD patterns during cooling at 2.5 °C/min from the isotropic melt. At 173 °C, a sudden shift of the halo *d* spacing occurs, implying the I → N phase transition. Another 2 °C decrease in temperature leads to the appearance of a narrow reflection peak at a 2θ of 19.0° and a smectic layer reflection at a 2θ of 4.0°. This can be assigned as a N → S_F phase transition, which is associated with the second high-temperature exothermic peak in the DSC cooling diagram as shown in Figure 2. The fiber pattern obtained at the same temperature demonstrates a monoclinic unit cell with $a = 1.28$ nm, $b = 0.53$ nm, $c = 3.10$ nm, and $\beta = 134°$. Upon further cooling, the lateral (110) reflection increases in intensity and reaches a maximum at approximately 110 °C. Additional cooling causes the intensities to start to increase for both the $(\bar{2}01)$ and (201) reflections, which are located on either side of the intense (110) reflection in quadrant. The

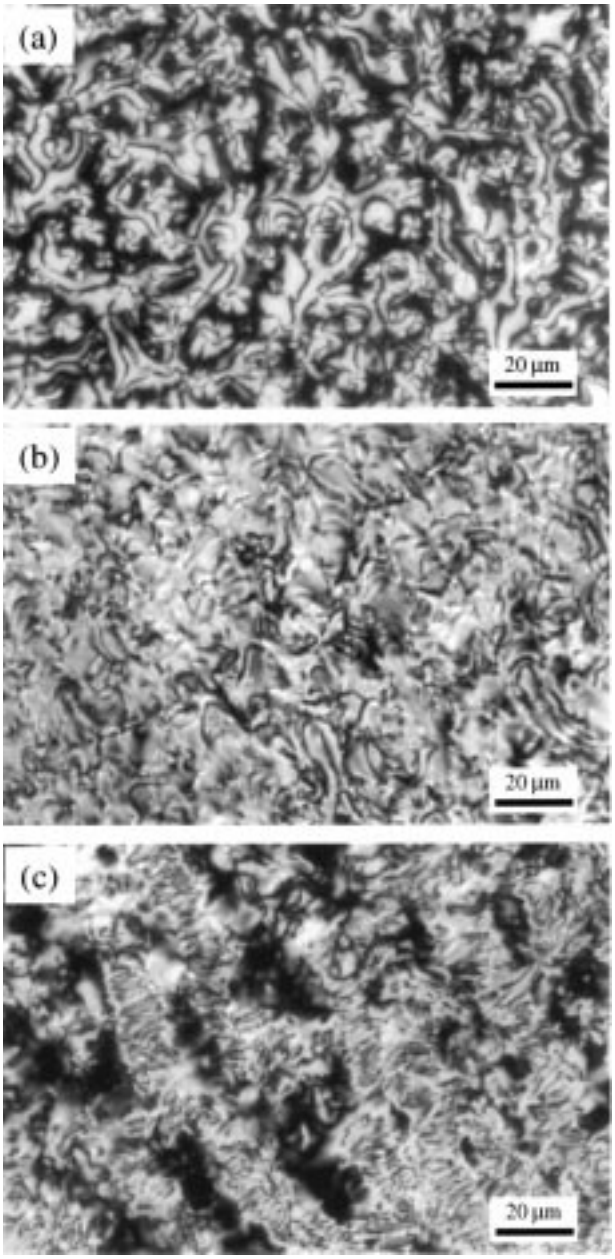

Figure 8. PLM observations in coTPP(7/12) at different temperatures: (a) 179 °C, (b) 169 °C, and (c) 159 °C.

(110) peak width at the half-height increases with decreasing temperature. This may represent a tendency for the (110) and (200) reflections to split due to a tiltingof the *c* axis of the monoclinic unit cell away from the alignment of the fiber direction.[1] This phase transition is assigned as a $S_F \rightarrow SC_G$ transition and can be recognized in a DSC cooling scan by a relatively broad but clear exothermic process.

Further experimental evidence supporting the $S_F \leftrightarrow SC_G$ transition in coTPP(11/12) is shown in Figure 10, which illustrates the linear dimensional change of the (110) *d* spacing with respect to temperature. The linear relationship between the *d* spacing and temperature exists below 80 °C and above 120 °C. The slopes, which represent the coefficients of thermal expansion for the lateral packing, are approximately 0.8 and 1.5×10^{-4} nm/°C, respectively. The slope change occurs between 80 and 120 °C. This corresponds to a thermodynamic first-order (perhaps, weak) transition as observed in the DSC cooling diagram (Figure 2). The transition sequence of coTPP(11/12) is determined:

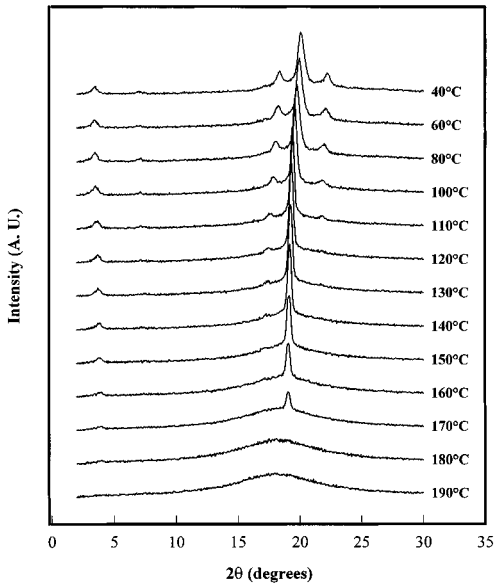

Figure 9. Set of WAXD powder patterns for coTPP(11/12) at different temperatures during cooling at 2.5 °C/min.

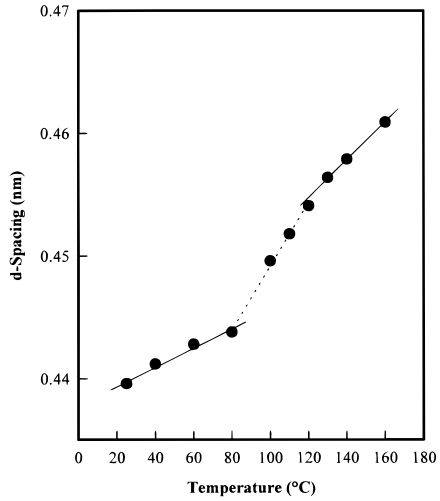

Figure 10. Change in (110) *d* spacing with respect to temperature for coTPP(11/12).

$$\text{glassy state} \leftrightarrow SC_G \leftrightarrow S_F \leftrightarrow N \leftrightarrow I$$

The layer spacing of coTPP(11/12) decreases with increasing temperature, contrary to the lateral thermal expansion. The reduced dimension along the chain direction is likely due to a transformation of the favorable low-temperature trans conformations of the methylene units into gauche conformations at higher temperatures. HomoTPPs exhibit this behavior as evidenced by the variable-temperature NMR results.[4]

The most interesting and challenging determination of the phase transition is in the case of coTPP(9/12). As previously discussed, an S_F phase can be identified for coTPP(9/12) at room temperature due to its hexagonal lateral packing and well-defined layer structure demonstrated by WAXD experiments. The $I \rightarrow N$ transition occurs at approximately 175 °C, at which point the scattering halo suddenly shifts, and the halo continues to narrow until a sharp Bragg reflection appears at 165 °C with a 2θ of 18.9° (*d* spacing of 0.47 nm) (Figure 11). Meanwhile, the low angle reflection is almost nonexist-

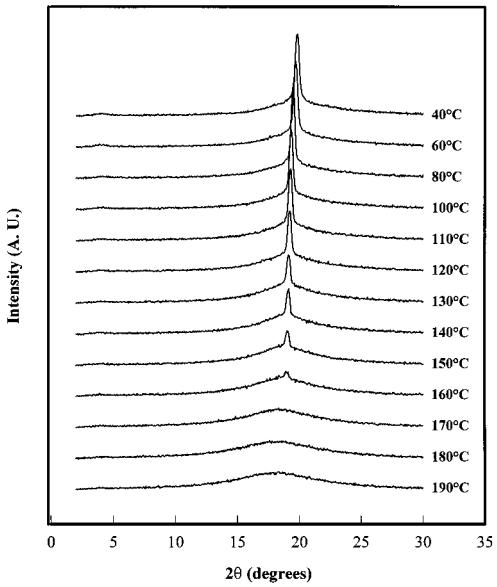

Figure 11. Set of WAXD powder patterns for coTPP(9/12) at different temperatures during cooling at 2.5 °C/min.

ent. Thus, a Φ_H phase is assigned. Upon further cooling, a weak layer reflection at a 2θ of 4.1° appears at approximately 100 °C. Figure 12 provides the magnified layer reflections of coTPP(9/12) WAXD fiber patterns in the transition temperature region. It is evident that the spotlike layer reflections at 90 °C change to the diffused streaks at 120 °C, indicating a decrease in the structural order along the layer normal direction. This transition is accompanied by a discontinuous change in the (110) *d* spacing as shown in Figure 13, which can be regarded as a thermodynamic weak first-order transition. However, this transition is very diffuse in DSC experiments. The transition is assigned as a $\Phi_H \leftrightarrow S_F$ transition, and the possible transition sequence of coTPP(9/12) is

$$\text{glassy state} \leftrightarrow S_F \leftrightarrow \Phi_H \leftrightarrow N \leftrightarrow I$$

Therefore, both the highly ordered smectic phase and the less ordered columnar phase are involved in a single copolymer.

It is observed from the WAXD experiments that the coTPPs(5/12 and 7/12) possess the narrow (110) lateral reflections in the Φ_H, and so does coTPP(9/12) in the Φ_H and S_F phases, with corresponding peak widths at half-heights smaller than those of the homoTPPs. This indicates that these coTPPs have larger correlation lengths within the two-dimensional lateral packing. It is also found that these lateral reflections gradually broaden upon cooling. Both observations may be associated with a slight tilting of the molecular orientation with respect to the fiber direction,[1] which could be caused by the competition between the formation of the layer and lateral orders. The methylene units may adjust their conformations, providing a more ordered packing in a lateral two-dimensional array at higher temperatures by sacrificing the layer order.

Thermodynamic Transition Properties. Thermodynamic transition properties such as transition temperatures and enthalpies can be analyzed following the identification of phase structures and transition sequences. On the basis of the exothermic peak separation results, the $I \leftrightarrow N$ transition for coTPPs(5/12, 7/12, 9/12, and 11/12) possess transition enthalpies of 10.1, 10.8, 11.7, and 12.4 kJ/mol, respectively, with corresponding equilibrium transition temperatures of 179, 182, 178, and 174 °C. Note that the contribution from the exotic N phase is included in these enthalpy values. However, TPP($n = 12$) has no N phase, but only an $I \leftrightarrow S_F$ transition having a transition enthalpy of 18.9 kJ/mol. In TPPs($n = 5$, 7, 9, and 11), the $I \leftrightarrow N$ transition enthalpies are 4.8, 6.0, 7.3, and 8.6 kJ/mol, respectively. Therefore, the enthalpies of the $I \leftrightarrow N$ transition in these coTPPs are lower than the average values of the corresponding homoTPPs, indicating that disorder is introduced by the dissimilarity of the methylene unit lengths in the comonomers. Note that these enthalpy changes follow a linear relationship with the number increase of the methylene units in the odd-numbered comonomers, which is similar to the previous observations in the homoTPPs[2,3] and other LC polymers.[19,20]

The $N \leftrightarrow \Phi_H$ transition enthalpies for coTPPs(5/12, 7/12, and 9/12) are 4.1, 5.7, and 6.7 kJ/mol, respectively, with corresponding transition temperatures of 157, 167, and 168 °C. The Φ_H transition enthalpies depend on the number of methylene units, indicating the influence of the methylene units on the development of structural order and transition behavior.

In coTPP(9/12), there is a very broad $\Phi_H \leftrightarrow S_F$ transition with an enthalpy of 0.9 kJ/mol, indicating the presence of a layered structure. The transition sequence of coTPP(11/12) follows the highly ordered smectic phases. Transition enthalpies of 7.3 and 5.3 kJ/mol are found for the $N \leftrightarrow S_F$ and $S_F \leftrightarrow SC_G$ transitions,

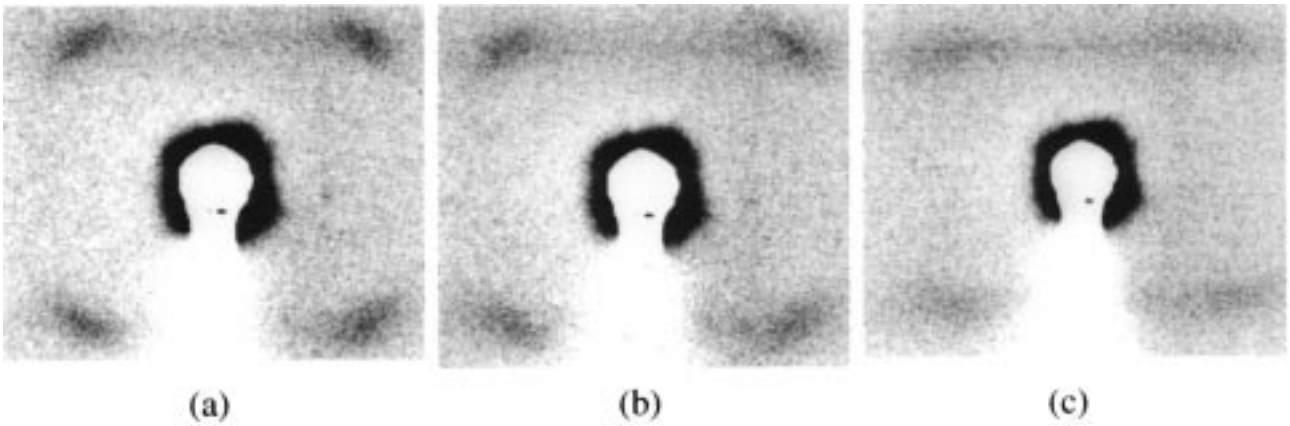

Figure 12. Layer structure change of coTPP(9/12) as shown in WAXD fiber patterns at different temperatures: (a) 90 °C, (b) 100 °C, and (c) 120 °C.

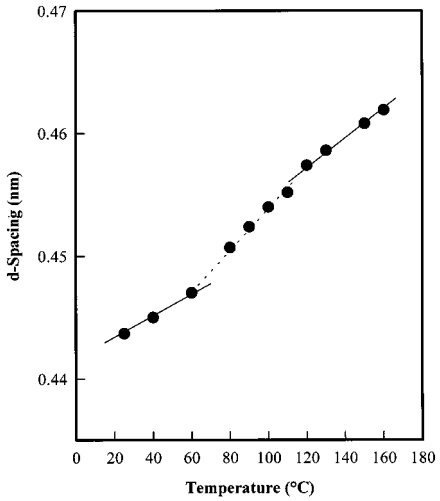

Figure 13. Change in (110) *d* spacing with respect to temperature for coTPP(9/12).

respectively, which are close to the corresponding average values of the TPPs(n = 11 and 12); the two transitions possess equilibrium temperatures of 173 and 110 °C, respectively.

Conclusions

In this series of coTPPs containing both odd- and even-numbered methylene units in equal molar composition, we have shown, for the first time, that when the numbers of methylene units in the comonomers are similar to each other, such as in coTPP(11/12), the phase structures and transition behaviors are similar to those in homoTPPs. However, when the difference between these two numbers increases, such as in coTPPs(5/12 and 7/12), the Φ_H phase can be identified. This phase is described as a two-dimensional lateral lattice array with disorder along the column direction. Furthermore, with an intermediate difference in methylene unit lengths, such as in coTPP(9/12), the structural change between Φ_H and S_F phases may occur.

Acknowledgment. This work was supported by the National Science Foundation (DMR-96-17030) and the Science and Technology Center for Advanced Liquid Crystal Optical Materials (ALCOM) at Kent State University, Case Western Reserve University, and the University of Akron. Support from the Chinese National Natural Science Foundation for promoting scientific collaborations is also acknowledged.

References and Notes

(1) Cheng, S. Z. D.; Yoon, Y.; Zhang, A.; Savitski, E. P.; Park, J.-Y.; Percec, V.; Chu, P. *Macromol. Rapid Commun.* **1995**, *16*, 533.
(2) Yoon, Y.; Zhang, A.; Ho, R.-M.; Cheng, S. Z. D.; Percec, V.; Chu, P. *Macromolecules* **1996**, *29*, 294.
(3) Yoon, Y.; Ho, R.-M.; Moon, B.; Kim, D.; McCreight, K. W.; Li, F.; Harris, F. W.; Cheng, S. Z. D.; Percec, V.; Chu, P. *Macromolecules* **1996**, *29*, 3421.
(4) Cheng, J.; Yoon, Y.; Ho, R.-M.; Leland, M.; Guo, M.; Cheng, S. Z. D.; Percec, V.; Chu, P. *Macromolecules* **1997**, *30*, 4688.
(5) Ho, R.-M.; Yoon, Y.; Leland, M.; Cheng, S. Z. D.; Yang, D.; Percec, V.; Chu, P. *Macromolecules* **1996**, *29*, 4528.
(6) Ho, R.-M.; Yoon, Y.; Lelend, M.; Cheng, S. Z. D.; Percec, V.; Chu, P. *Macromolecules* **1997**, *30*, 3349.
(7) Malthete, J.; Levelut, A. M. *Mol. Cryst. Liq. Cryst.* **1981**, *71*, 111.
(8) Levelut, A. M.; Malthete, J. *Mol. Cryst. Liq. Cryst.* **1984**, *106*, 121.
(9) De Genes, P. G.; Prost, J. *The Physics of Liquid Crystals*; Oxford: New York, 1993.
(10) Malthete, J.; Levelut, A. M.; Tinh, N. H. *J. Phys. Lett.* **1985**, *46*, 875.
(11) Destrade, C.; Tinh, N. H.; Roubineau, A.; Levelut, A. M. *Mol. Cryst. Liq. Cryst.* **1988**, *159*, 163.
(12) Unger, G.; Feijoo, J. L.; Percec, V.; Yourd, R. *Macromolecules* **1991**, *24*, 953.
(13) Ungar, G. *Polymer* **1993**, *34*, 2050.
(14) Percec, V.; Chu, P.; Ungar, G.; Cheng, S. Z. D.; Yoon, Y. *J. Mater. Chem.* **1994**, *4*, 719.
(15) Pershan, P. S. *Structure of Liquid Crystal Phases*; World Scientific: Singapore, 1988.
(16) Yandrasits, A.; Cheng, S. Z. D.; Zhang, A.; Cheng. J.; Wunderlich, B.; Percec, V. *Macromolecules* **1992**, *25*, 2112.
(17) Pardey, Harris, F. W.; Cheng, S. Z. D.; Adduci, J.; Facinelli, J. V.; Lenz, R. W. *Macromolecules* **1992**, *25*, 5060.
(18) Pardey, R.; Shen, D.; Gabori, P. A.; Harris, F. W.; Cheng, S. Z. D.; Adduci, J.; Facinelli, J. V.; Lenz, R. W. *Macromolecules* **1993**, *26*, 3687.
(19) Blumstein, A.; Thomas, O. *Macromolecules* **1982**, *15*, 1264.
(20) Blumstein, B.; Blumstein, A. *Mol. Cryst. Liq. Cryst.* **1988**, *165*, 361.

MA9818782